Optics Communications 368 (2016) 129–133

Contents lists available at ScienceDirect

Optics Communications

journal homepage: www.elsevier.com/locate/optcom

Transient gain–absorption of the probe field in triple quantum dots coupled by double tunneling

Si-Cong Tian [a], Xiao-Jun Zhang [c], Ren-Gang Wan [d], Shuai Zhao [b], Hao Wu [a], Shi-Li Shu [a], Li-Jie Wang [a], Cun-Zhu Tong [a,*]

[a] State Key laboratory of Luminescence and Applications, Changchun Institute of Optics, Fine Mechanics and Physics, Chinese Academy of Sciences, Changchun 130033, China
[b] State Key Laboratory of Laser Interaction with Matter, Changchun Institute of Optics, Fine Mechanics and Physics, Chinese Academy of Sciences, Changchun 130033, China
[c] Changchun Observatory, National Astronomical Observatories, CAS, Changchun 130117, China
[d] School of Physics and Information Technology, Shaanxi Normal University, Xi'an 710062, China

ARTICLE INFO

Article history:
Received 20 November 2015
Received in revised form
14 January 2016
Accepted 5 February 2016
Available online 12 February 2016

Keywords:
Triple quantum dots
Electromagnetically induced transparency
Transient evolution

ABSTRACT

The transient gain–absorption property of the probe field in a linear triple quantum dots coupled by double tunneling is investigated. It is found that the additional tunneling can dramatically affect the transient behaviors under the transparency condition. The dependence of transient behaviors on other parameters, such as probe detuning, the pure dephasing decay rate of the quantum dots and the initial conditions of the population, are also discussed. The results can be explained by the properties of the dressed states generated by the additional tunneling. The scheme may have important application in quantum information network and communication.

1. Introduction

The phenomenon of electromagnetically induced transparency (EIT), which bases on the laser induced atomic coherence, plays an important role in the interaction between light and matter [1–3]. Possible applications of EIT include slow [4–6] and fast light [7], storage of Light [8,9] and optical quantum memory [10]. And transient properties of EIT in three-level atomic systems are widely studied [11–16], because of their potential application in an optical switch [17,18]. Moreover, transient properties in four-level atomic systems [19–21], in the atomic system with spontaneously generated coherence (SGC) effect [22–24] or near a plasmonic nanostructure [25], in quantum dots (QDs) [26] and quantum wells (QWs) [27,28] are also studied.

On the other hand, double quantum dots (DQDs) are received extensive concern nowadays. By the self assembled dot growth method, DQDs can be fabricated [29]. The experimental works show that in DQDs an external electric can control the interdot electron tunneling [30] and the exciton fine structure [31]. Meanwhile, other theoretical works of DQDs such as EIT and slow light [32–34], electron tunneling [35–37], optical bistability [38,39], narrowing of fluorescence spectrum [40] are studied. Furthermore, triple quantum dots (TQDs) have been fabricated in much experimental progress [41]. Theoretical works of TQDs, such as transmission-dispersion spectrum [42], optical switch [43], resonance fluorescence spectrum [44], Kerr nonlinearity [45], optical bistability [46] and entanglement [47] are studied.

The transient gain–absorption property in DQDs has been investigated recently [48], but to our knowledge there is no investigation on transient gain–absorption property in TQDs. In this paper, we analyze the transient gain–absorption property in TQDs under double tunneling couplings. By applying the additional tunneling, the transient gain–absorption property of the probe field can be efficiently modified. The use of additional tunneling can drive the four-level TQDs system into double Λ-type configuration, which is responsible for the corresponding results. And also the impact of other parameters on the transient behavior are investigated, such as the probe detuning, the pure dephasing decay rate of the quantum dots and the initial conditions of the population. The paper is organized as followed: in Section 2, the model and the basic equations of TQDs are given. In Section 3 the numerical results and explanations are shown. Section 4 is the

* Corresponding author.
E-mail addresses: tiansicong@ciomp.ac.cn (S.-C. Tian), tongcz@ciomp.ac.cn (C.-Z. Tong).

http://dx.doi.org/10.1016/j.optcom.2016.02.010
0030-4018/

conclusions.

2. Models and equations

We consider the TQDs consisted by three vertically (in the growth direction) stacked self-assembled InAs QDs, as shown in Fig. 1(a). The QDs are grown with thin tunnel barrier of GaAs/AlGaAs, thus the electrons can coherently tunnel between the three dots. By controlling thicknesses of the QDs, the QDs can have different optical transition energies and can be optically addressable with a resonant laser frequency. And the QDs are incorporated into a Schottky diode, so that by adjusting the voltage bias each QD is charged with a single electron.

When the voltage bias is not applied, the conduction-band electron energy levels are out of resonance, therefore, the electron tunneling between the neighbor QDs is quite weak. On the contrary, when the gate voltage is applied, the conduction-band electron energy levels are on resonance, therefore, the electron tunneling between the neighbor QDs becomes very strong. The hole tunneling is neglected due to the off-resonance of the valence-band energy levels in the latter situation.

Under the resonant coupling of a probe laser field with QD1, an electron is excited in QD1. Then with the tunneling, the electron can be transferred to QD2 and QD3. Thus the TQDs structure can be treated as a four-level system (Fig. 1(b)): the ground level $|0\rangle$, where there is no excitations in any QDs, the direct exciton level $|1\rangle$, where the electron and hole are both in the first QD, the indirect exciton level $|2\rangle$, where the electron is in the second dot and the hole remains in the first dot, and the indirect exciton level $|3\rangle$, where the electron is in the third dot and the hole remains in the first dot.

The Hamiltonian in the frame rotating with double tunneling couplings is of the form

$$H = \begin{pmatrix} 0 & -\Omega_p & 0 & 0 \\ -\Omega_p & \delta_p & -T_1 & 0 \\ 0 & -T_1 & \delta_p - \omega_{12} & -T_2 \\ 0 & 0 & -T_2 & \delta_p - \omega_{12} - \omega_{23} \end{pmatrix}. \tag{1}$$

Here $\Omega_p = \mu_{01} E_p$ is the Rabi frequency of the probe field, where E_p denotes the electric field amplitude, and $\mu_{01} = \boldsymbol{\mu}_{01} \cdot \mathbf{e}$ denotes the electric dipole moment of transition $|0\rangle \leftrightarrow |1\rangle$. ($\mathbf{e}$ is the polarization vector.) And $\delta_p = \omega_{10} - \omega_p$ is the detuning of the probe field, with ω_p being the frequency of the probe field and ω_{10} being the frequency of the transition $|1\rangle \leftrightarrow |0\rangle$. T_1 and T_2 are the intensities of the tunneling couplings, which depend on the intrinsic sample barrier and the external electric field. ω_{12} and ω_{23} are the energy splittings of the excited states, which depend on the effective confinement potential. And we should mention that, in experiments the confined Stark effect induced by the external electric field will shift the energy levels of each dot, therefore, there is a slight external electric field dependence on the parameters ω_{12} and ω_{23}. But such effect can be easily compensated during system characterization [35].

The dynamics of the system is described by Liouville–von Neumman–Lindblad equation

$$\frac{d\rho}{dt} = -\frac{i}{\hbar}[H, \rho(t)] + L(\rho). \tag{2}$$

Here $\rho(t)$ is the density-matrix operator. The Liouville operator $L(\rho)$ describes the dissipative process. With the Markovianapproximation, Liouville operator can be written as

$$L(\rho) = \frac{1}{2}\sum_i \Gamma_{ij}(2|j\rangle\langle i|\rho|i\rangle\langle j| - \rho|i\rangle\langle i| - |i\rangle\langle i|\rho) + \gamma_{i0}^d(2|i\rangle\langle i|\rho|i\rangle\langle i| - \rho|i\rangle\langle i| - |i\rangle\langle i|\rho), \tag{3}$$

where the first term describes the spontaneous decay process $|i\rangle \to |j\rangle$ and the second term is the pure dephasing with rate γ_{i0}^d.

Substituting Eqs. (1) and (3) into Eq. (2), then the dynamics of the system is described by the following density matrix equations:

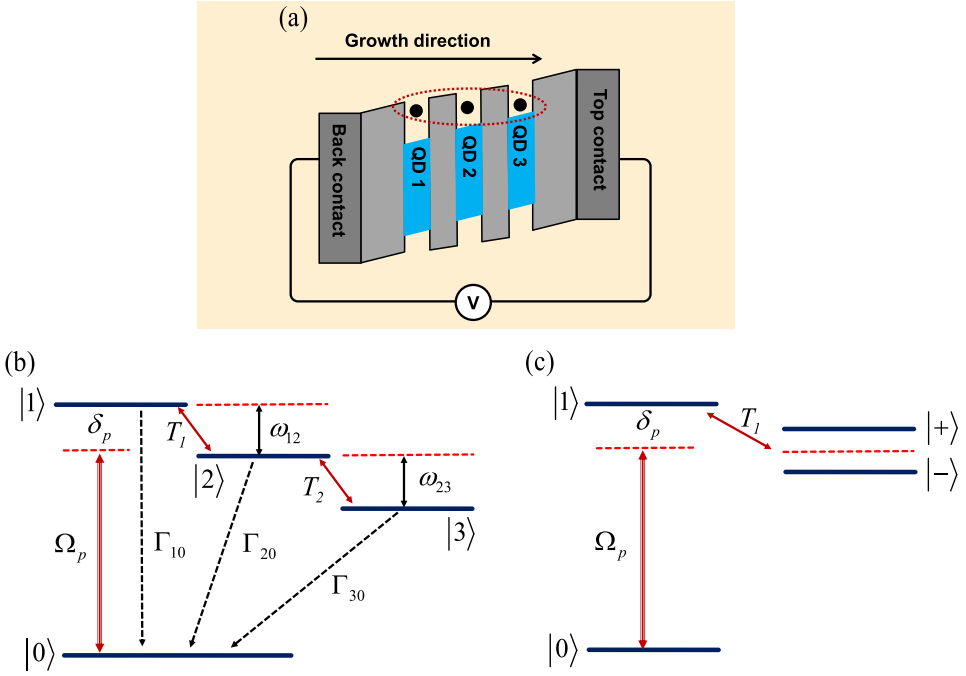

Fig. 1. (a) The schematic energy diagram of the TQDs system. (b) The schematic of the level configuration of a TQD system. (c) The partially dressed state of the TQD system under the tunneling T_2.

$$\dot{\rho}_{01} = i\Omega_p(\rho_{11} - \rho_{00}) - iT_1\rho_{02} + \left[i\delta_p - \left(\frac{\Gamma_{10}}{2} + \gamma_{10}^d\right)\right]\rho_{01}, \tag{4a}$$

$$\dot{\rho}_{02} = i\Omega_p\rho_{12} - iT_1\rho_{01} - iT_2\rho_{03} + \left[i(\delta_p - \omega_{12}) - \left(\frac{\Gamma_{20}}{2} + \gamma_{20}^d\right)\right]\rho_{02}, \tag{4b}$$

$$\dot{\rho}_{03} = i\Omega_p\rho_{13} - iT_2\rho_{02} + \left[i(\delta_p - \omega_{12} - \omega_{23}) - \left(\frac{\Gamma_{30}}{2} + \gamma_{30}^d\right)\right]\rho_{03}, \tag{4c}$$

$$\dot{\rho}_{11} = i\Omega_p(\rho_{01} - \rho_{10}) + iT_1(\rho_{21} - \rho_{12}) - \Gamma_{10}\rho_{11}, \tag{4d}$$

$$\dot{\rho}_{12} = i\Omega_p\rho_{02} + iT_1(\rho_{22} - \rho_{11}) - iT_2\rho_{13} - \left[i\omega_{12} + \left(\frac{\Gamma_{10} + \Gamma_{20}}{2} + \gamma_{10}^d + \gamma_{20}^d\right)\right]\rho_{12}, \tag{4e}$$

$$\dot{\rho}_{13} = i\Omega_p\rho_{03} + iT_1\rho_{23} - iT_2\rho_{12} - \left[i(\omega_{12} + \omega_{23}) + \left(\frac{\Gamma_{10} + \Gamma_{30}}{2} + \gamma_{10}^d + \gamma_{30}^d\right)\right]\rho_{13}, \tag{4f}$$

$$\dot{\rho}_{22} = iT_1(\rho_{12} - \rho_{21}) + iT_2(\rho_{32} - \rho_{23}) - \Gamma_{20}\rho_{22}, \tag{4g}$$

$$\dot{\rho}_{23} = iT_1\rho_{13} + iT_2(\rho_{33} - \rho_{22}) - \left[i\omega_{23} + \left(\frac{\Gamma_{20} + \Gamma_{30}}{2} + \gamma_{20}^d + \gamma_{30}^d\right)\right]\rho_{23}, \tag{4h}$$

$$\dot{\rho}_{33} = iT_2(\rho_{23} - \rho_{32}) - \Gamma_{30}\rho_{33}, \tag{4i}$$

with $\rho_{00} + \rho_{11} + \rho_{22} + \rho_{33} = 1$ and $\dot{\rho}_{ij} = \dot{\rho}_{ji}{}^*(i, j = 0, 1, 2, 3)$.

As we known, the gain–absorption properties for the probe field on the transition $|1\rangle \leftrightarrow |0\rangle$ is determined by the imaginary part of ρ_{10}, in the limit of the weak intensity of the probe. And we only focus on the time evolution of the gain–absorption properties. In the following section, we will give some results for transient $\mathrm{Im}(\rho_{10})$ by solving Eq. (4) for several parameters of TQDs. For our investigation, the realistic parameters are according to Ref. [45], and can be summarized as Ω_p~0 − 0.1 μeV/ħ, T_1, T_2~10 − 100 μeV/ħ, ω_{12}, ω_{23}~−30 − 30 μeV/ħ, Γ_{10}~0 − 6.6 μeV/ħ, $\Gamma_{20} = \Gamma_{30} = 10^{-4}\Gamma_{10}$, γ_{10}^d~0 − 6.6 μeV/ħ, and $\gamma_{20}^d = \gamma_{30}^d = 10^{-3}\gamma_{10}^d$.

3. Results and discussions

First, with $\omega_{12} = \omega_{23} = 0$, we plot in Fig. 2 the time evolution of $\mathrm{Im}(\rho_{10})$ for fixed zero probe detuning and varying the intensity of tunneling T_2. And in our calculations, all the parameters are scaled by $\Gamma_{10} = 6.6$ μeV/ħ, thus $\delta_p = 0$, $\Omega_p = 0.01\Gamma_{10}$, $T_1 = 2\Gamma_{10}$, $\Gamma_{20} = \Gamma_{30} = 10^{-4}\Gamma_{10}$, $\gamma_{10}^d = 0.5\Gamma_{10}$, $\gamma_{20}^d = \gamma_{30}^d = 0.5 \times 10^{-3}\Gamma_{10}$. When the intensity of the tunneling T_2 is set to zero, $\mathrm{Im}(\rho_{10})$ exhibits periodic absorption and gain, and eventually goes to zero steady-state value ($\mathrm{Im}(\rho_{10}) = 0$). Then when tunneling T_2 is increased to a small value, i.e., $T_2 = 0.5\Gamma_{10}$, the amplitude of the transient probe gain is reduced, and $\mathrm{Im}(\rho_{10})$ goes to a positive value and eventually reaches nonzero steady-state value. With increasing intensity of T_2, the oscillation frequency of $\mathrm{Im}(\rho_{10})$ speeds up. Begins with the second oscillation period, $\mathrm{Im}(\rho_{10})$ goes to a positive value rapidly, and transient gain is eliminated completely. At last $\mathrm{Im}(\rho_{10})$ reaches the same maximum absorption value with less time. Compared with the case of $T_2 = 0$, the most significant characters for $T_2 \neq 0$ is

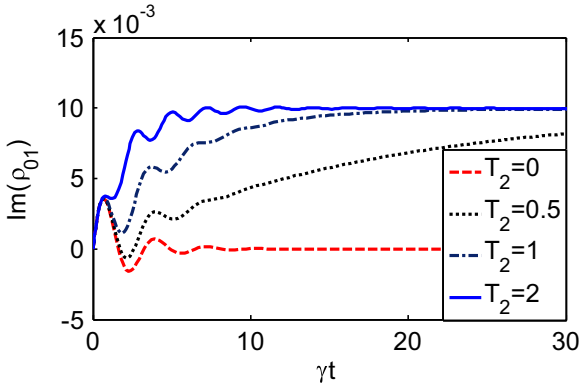

Fig. 2. The time evolution of $\mathrm{Im}(\rho_{10})$ for varying tunneling intensity T_2 under the resonant tunneling coupling ($\omega_{12} = \omega_{23} = 0$). The initial conditions of the population are $\rho_{00}(0) = 1$, and other $\rho_{ij}(0) = 0(i, j = 0 - 3)$. All the parameters are scaled by $\Gamma_{10} = 6.6$ μeV/ħ, and $\delta_p = 0$, $\Omega_p = 0.01\Gamma_{10}$, $T_1 = 2\Gamma_{10}$, $\Gamma_{20} = \Gamma_{30} = 10^{-4}\Gamma_{10}$, $\gamma_{10}^d = 0.5\Gamma_{10}$, $\gamma_{20}^d = \gamma_{30}^d = 0.5 \times 10^{-3}\Gamma_{10}$.

that, $\mathrm{Im}(\rho_{10})$ will reach the same maximum positive steady-state value (absorption). That is, the coupling of tunneling T_2 will lead to the disappearance of the transparency of the steady-state of the transient $\mathrm{Im}(\rho_{10})$ for zero probe detuning. (From dotted line in Fig. 2, the steady-state value is smaller than other two cases. But it will reach the same maximum absorption value at last.)

We can see the above results in the dressed state picture clearly. With only one tunneling T_1, the system is similar to a three-level Λ type system. When $\omega_{12} = 0$ and $\delta_p = 0$, the transparency condition is obtained, and the probe field is transparent to the medium. As a result, the probe field will reach the steady-state value $\mathrm{Im}(\rho_{10}) = 0$ at last. Then with the additional tunneling T_2, the state $|2\rangle$ splits into two partially dressed states $|+\rangle = \cos\theta^*|2\rangle - \sin\theta|3\rangle$ and $|-\rangle = \sin\theta|2\rangle + \cos\theta|3\rangle$, where $\tan\theta = \left(\omega_{23} + \sqrt{\omega_{23}^2 + 4T_2^2}\right)/2T_2$, thus two Λ type systems show up (Fig. 1(c)). When $\omega_{12} = 0$, the tunneling T_1 is nonresonant with neither of the transition $|1\rangle \leftrightarrow |+\rangle$ nor $|1\rangle \leftrightarrow |-\rangle$. For $\delta_p = 0$, the transparency condition is not satisfied, therefore, the probe field is absorpted by the medium. As a consequence, the probe field will reach the steady-state with the maximum absorption value.

Next, still with $\omega_{12} = \omega_{23} = 0$, we plot the time evolution of $\mathrm{Im}(\rho_{10})$ for nonresonant probe field in Fig. 3. For $\delta_p = \pm T_2$, except for the first oscillation period, $\mathrm{Im}(\rho_{10})$ dropped down rapidly. And $\mathrm{Im}(\rho_{10})$ exhibits transient absorption and gain during the transient process. At last $\mathrm{Im}(\rho_{10})$ reaches the zero steady-state value ($\mathrm{Im}(\rho_{10}) = 0$). These properties are quite different from the case of $\delta_p = 0$ and can also be understood in the dressed state picture. As

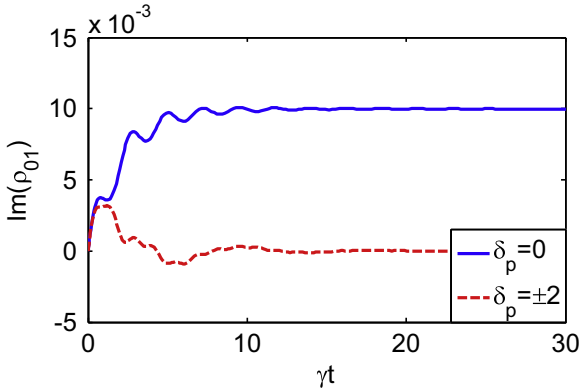

Fig. 3. The time evolution of $\mathrm{Im}(\rho_{10})$ for varying probe detuning δ_p under the resonant tunneling coupling ($\omega_{12} = \omega_{23} = 0$). Other parameters are the same as those used in Fig. 2, except that $T_2 = 2\Gamma_{10}$.

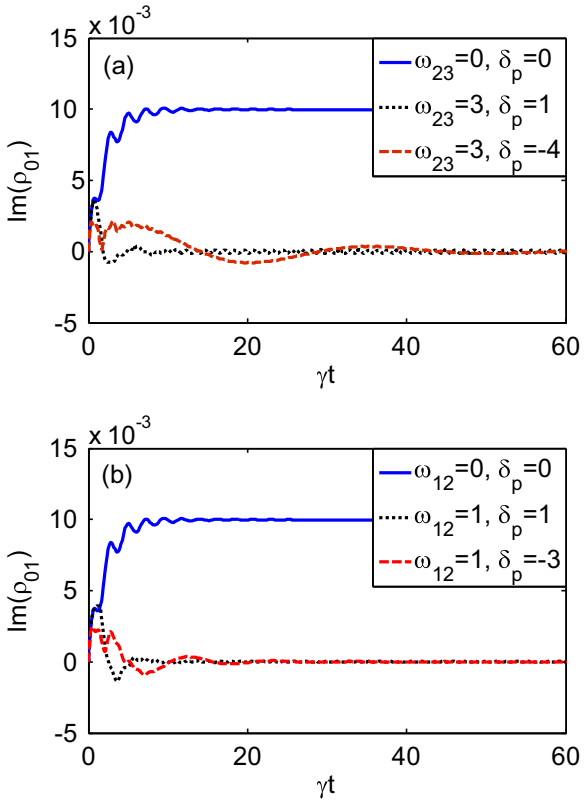

Fig. 4. The time evolution of $\mathrm{Im}(\rho_{10})$ for varying probe detuning δ_p under the nonresonant tunneling coupling($\omega_{12} \neq 0$or$\omega_{23} \neq 0$). (a) $\omega_{12} = 0$, (b) $\omega_{23} = 0$. Other parameters are the same as those used in Fig. 2, except that $T_2 = 2\Gamma_{10}$.

discussed above, under the coupling of tunneling T_2, the state $|2\rangle$ splits into two dressed states $|+\rangle$ and $|-\rangle$. For $\omega_{23} = 0$, the detuning between the tunneling T_1 and the transition of $|1\rangle \leftrightarrow |+\rangle$ or $|1\rangle \leftrightarrow |-\rangle$ is $\pm T_2$. So when $\delta_p = \pm T_2$, the transparency condition is established in one of the two Λ type systems, and the probe field will be transparent to the medium. As a result, $\mathrm{Im}(\rho_{10})$ will reach the zero steady-state value at last.

The above results are obtained under the condition of $\omega_{12} = \omega_{23} = 0$. To be more general, we consider the cases of the nonresonance tunneling coupling. As can be easily obtained, the transparency condition can be established if the detuning of the probe field is tuned to $\delta_{dark} = -\omega_{12} + \left(-\omega_{23} \pm \sqrt{\omega_{23}^2 + 4T_2^2}\right)/2$. This means the probe field will propagate through the medium without any absorption, in the condition that the probe detuning is tuned to δ_{dark}. In Fig. 4 we plot the time evolution of $\mathrm{Im}(\rho_{10})$ for $\omega_{12} \neq 0$ or $\omega_{23} \neq 0$. As can be seen, when $\delta_p = \delta_{dark}$, except for the first oscillation period, $\mathrm{Im}(\rho_{10})$ dropped down rapidly. And $\mathrm{Im}(\rho_{10})$ exhibits transient absorption and gain during the transient process. At last $\mathrm{Im}(\rho_{10})$ reaches the zero steady-state value ($\mathrm{Im}(\rho_{10}) = 0$). These results are coinciding with the discussion above.

As we known, the pure dephasing decay rate, which is due to the coupling with the photons and the acoustic phonons, will increase with the increasing temperature. So next we will discuss the impact of the pure dephasing decay rate on transient behaviors of $\mathrm{Im}(\rho_{10})$. In Fig. 5, we plot the time evolution of $\mathrm{Im}(\rho_{10})$ for different value of γ_{10}^d. When no pure dephasing decay rate is taken into, i.e. $\gamma_{10}^d = 0$, $\mathrm{Im}(\rho_{10})$ exhibits absorption without any gain in the whole process. The transient absorption oscillates and eventually reaches a nonzero steady-state value. As γ_{10}^d is increasing, $\mathrm{Im}(\rho_{10})$ still oscillates above the zero value and exhibits absorption without any gain. But the oscillatory frequency of the transient

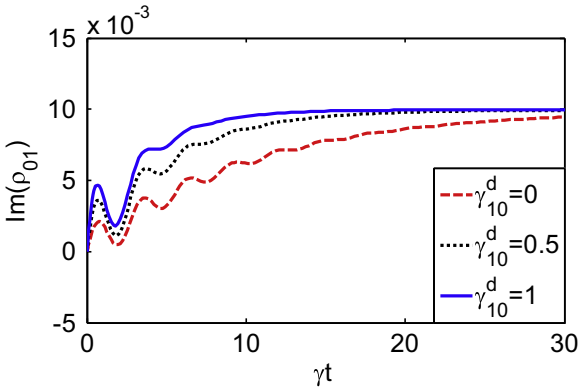

Fig. 5. The time evolution of $\mathrm{Im}(\rho_{10})$ for varying pure dephasing decay rate γ_{10}^d. Other parameters are the same as those used in Fig. 2, except that $T_2 = \Gamma_{10}$.

absorption is reduced, and the transient absorption oscillates fewer periods and takes less time to reach the steady-state value. And further, the transient absorption will reach the same steady-state value at last.

Last we will see the impact of initial conditions of the population on transient behavior of $\mathrm{Im}(\rho_{10})$ and show the corresponding results in Fig. 6. First when all the population is distributed in the ground state $|0\rangle$, that is $\rho_{00}(0) = 1$, and other $\rho_{ij}(0) = 0 (i, j = 0 - 3)$, the probe field oscillates and exhibits absorption without any gain in the entire process, and reaches a positive steady-state value eventually. Then when both the ground state $|0\rangle$ and the excited state $|1\rangle$ have the same population, i.e. $\rho_{00}(0) = \rho_{11}(0) = 0.5$, and other $\rho_{ij}(0) = 0 (i, j = 0 - 3)$, the circumstance is similar to the above case, but the transient absorption spends more time to reach the same steady-state value. Last when all the population is pumped to the excited state $|1\rangle$, such as $\rho_{11}(0) = 1$, and other $\rho_{ij}(0) = 0 (i, j = 0 - 3)$, the period of oscillations of $\mathrm{Im}(\rho_{10})$ is increased observably, and the time for $\mathrm{Im}(\rho_{10})$ to reach the same steady-state value continues increasing. In addition, the most important characteristic is that $\mathrm{Im}(\rho_{10})$ exhibits periodic absorption and gain during the first several periods of oscillations.

4. Conclusions

In conclusion, we have theoretically investigated the transient gain–absorption properties of the probe field in the four-level TQDs coupled by double tunneling. We find that the intensity of the additional tunneling affects the transient behavior under the transparency condition. We also find that the transient behavior

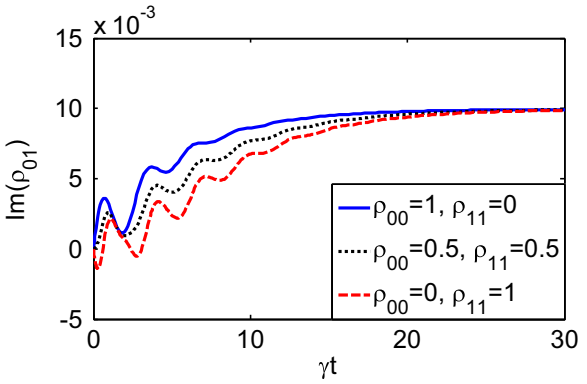

Fig. 6. The time evolution of $\mathrm{Im}(\rho_{10})$ for varying initial conditions of the population. Other parameters are the same as those used in Fig. 2, except that $T_2 = \Gamma_{10}$.

relies on other parameters, such as the probe detuning, the pure dephasing decay rate of the quantum dots and the initial conditions of the population. And we explain the corresponding results in the dressed state picture under the additional tunneling coupling. Compared with the studies in the atomic system [11–21], the study in TQDs is more practical, because that TQDs has advantage of customized design and ease of integration, and no coupling field is needed in the system. Therefore, it may provide some new possibilities for technological applications in quantum information network and communication.

Acknowledgments

This work is supported by the financial support from the National Natural Science Foundation of China (Grant nos. 11304308, 11204029, 61176046 and 61306086), the National Basic Research Program of China (Grant nos. 2013CB933300), the International Science Technology Cooperation Program of China (Grant no. 2013DFR00730), Jilin Provincial Natural Science Foundation (Grant nos. 20140101203JC and 20140520127JH).

References

[1] S.E. Harris, Phys. Today 50 (1997) 36–42.
[2] J.P. Marangos, J. Mod. Opt. 45 (1998) 471–503.
[3] M. Fleischhauer, A. Imamoglu, J.P. Marangos, Rev. Mod. Phys. 77 (2005) 633–673.
[4] S.E. Harris, L.V. Hau, Phys. Rev. Lett. 82 (1999) 4611–4614.
[5] L.V. Hau, S.E. Harris, Z. Dutton, C.H. Behroozi, Nature 397 (1999) 594–598.
[6] M.M. Kash, V.A. Sautenkov, A.S. Zibrov, L. Hollberg, G.R. Welch, M.D. Lukin, Y. Rostovtsev, E.S. Fry, M.O. Scully, Phys. Rev. Lett. 82 (1999) 5229–5232.
[7] L.J. Wang, A. Kuzmich, A. Dogariu, Nature 406 (2000) 277–279.
[8] C. Liu, Z. Dutton, C.H. Behroozi, L.V. Hau, Nature 409 (2001) 490–493.
[9] D.F. Phillips, A. Fleischhauer, A. Mair, R.L. Walsworth, M.D. Lukin, Phys. Rev. Lett. 86 (2001) 783–786.
[10] A.I. Lvovsky, B.C. Sanders, W. Tittel, Nat Photon 3 (2009) 706–714.
[11] Y.-Q. Li, M. Xiao, Opt. Lett. 20 (1995) 1489–1491.
[12] Y. Zhu, Phys. Rev. A 53 (1996) 2742–2747.
[13] Y. Zhu, Phys. Rev. A 55 (1997) 4568–4575.
[14] H.X. Chen, A.V. Durrant, J.P. Marangos, J.A. Vaccaro, Phys. Rev. A 58 (1998) 1545–1548.
[15] A.D. Greentree, T.B. Smith, S.R. de Echaniz, A.V. Durrant, J.P. Marangos, D. M. Segal, J.A. Vaccaro, Phys. Rev. A 65 (2002) 053802.
[16] P. Valente, H. Failache, A. Lezama, Phys. Rev. A 65 (2002) 023814.
[17] Y.-F. Chen, G.-C. Pan, I.A. Yu, Phys. Rev. A 69 (2004) 063801.
[18] A.M.C. Dawes, L. Illing, S.M. Clark, D.J. Gauthier, Science 308 (2005) 672–674.
[19] J.-Q. Shen, Z.-C. Ruan, S. He, Phy. Lett. A 330 (2004) 487–495.
[20] M. Sahrai, M. Mahmoudi, R. Kheradmand, Phy. Lett. A 367 (2007) 408–414.
[21] J.Q. Shen, New J. Phys. 9 (2007) 374.
[22] W.-H. Xu, J.-H. Wu, J.-Y. Gao, Phys. Rev. A 66 (2002) 063812.
[23] M. Sahrai, M. Mahmoudi, J. Phys. B-At. Mol. Opt. Phys. 42 (2009) 235503.
[24] S.-C. Tian, C.-Z. Tong, R.-G. Wan, Y.-Q. Ning, L. Qin, Y. Liu, L.-J. Wang, H. Zhang, Z.-B. Wang, J.-Y. Gao, Chin. Phys. B 23 (2014) 044205.
[25] S. Evangelou, V. Yannopapas, E. Paspalakis, Opt. Commun. 314 (2014) 36–40.
[26] S. Marcinkevičius, A. Gushterov, J.P. Reithmaier, Appl. Phys. Lett. 92 (2008) 041113.
[27] Z. Wang, Opt. Commun. 283 (2010) 2552–2556.
[28] Z. Wang, Physica E 43 (2011) 1329–1333.
[29] L. Wang, A. Rastelli, S. Kiravittaya, M. Benyoucef, O.G. Schmidt, Adv. Mater. 21 (2009) 2601–2618.
[30] K. Müller, A. Bechtold, C. Ruppert, M. Zecherle, G. Reithmaier, M. Bichler, H. J. Krenner, G. Abstreiter, A.W. Holleitner, J.M. Villas-Boas, M. Betz, J.J. Finley, Phys. Rev. Lett. 108 (2012) 197402.
[31] N. Sköld, A. Boyer de la Giroday, A.J. Bennett, I. Farrer, D.A. Ritchie, A.J. Shields, Phys. Rev. Lett. 110 (2013) 016804.
[32] C.-H. Yuan, K.-D. Zhu, Appl. Phys. Lett. 89 (2006) 052115.
[33] H.S. Borges, L. Sanz, J.M. Villas-Bôas, O.O. Diniz Neto, A.M. Alcalde, Phys. Rev. B 85 (2012) 115425.
[34] S. Michael, W.W. Chow, H.C. Schneider, Phys. Rev. B 88 (2013) 125305.
[35] J.M. Villas-Bôas, A.O. Govorov, S.E. Ulloa, Phys. Rev. B 69 (2004) 125342.
[36] S.G. Kosionis, A.F. Terzis, E. Paspalakis, Phys. Rev. B 75 (2007) 193305.
[37] H.S. Borges, L. Sanz, J.M. Villas-Bôas, A.M. Alcalde, Phys. Rev. B 81 (2010) 075322.
[38] Z. Wang, S. Zhen, X. Wu, J. Zhu, Z. Cao, B. Yu, Opt. Commun. 304 (2013) 7–10.
[39] H. Jafarzadeh, M. Sahrai, K. Jamshidi-Ghaleh, Eur. Phys. J. D 68 (2014) 115.
[40] S.-C. Tian, C.-Z. Tong, C.-L. Wang, L.-J. Wang, H. Wu, E.-B. Xing, Y.-Q. Ning, L.-J. Wang, Opt. Commun. 312 (2014) 296–301.
[41] H. Chang-Yu, S. Yun-Pil, K. Marek, H. Pawel, Rep. Prog. Phys. 75 (2012) 114501.
[42] R. Yu, J. Li, C. Ding, X. Yang, Phy. Lett. A 375 (2011) 2738–2746.
[43] M. Sahrai, M.R. Mehmannavaz, H. Sattari, Appl. Opt. 53 (2014) 2375–2383.
[44] S.-C. Tian, C.-Z. Tong, C.-L. Wang, Y.-Q. Ning, J. Lumin. 153 (2014) 169–176.
[45] S.-C. Tian, R.-G. Wan, C.-Z. Tong, Y.-Q. Ning, L. Qin, Y. Liu, J. Opt. Soc. Am. B 31 (2014) 1436–1442.
[46] S.-C. Tian, R.-G. Wan, C.-Z. Tong, Y.-Q. Ning, J. Opt. Soc. Am. B 31 (2014) 2681–2688.
[47] M. Sahrai, B. Arzhang, D. Taherkhani, V.T.A. Boroojerdi, Physica E 67 (2015) 121–127.
[48] M. Ioannou, J. Boviatsis, E. Paspalakis, Physica E 40 (2008) 2010–2012.